PRECISION MEASUREMENT OF $e^+e^- \to \mu\mu\gamma$ AND $e^+e^- \to \pi\pi\gamma$ CROSS SECTIONS WITH THE KLOE DETECTOR

C. BLOISE on behalf of the KLOE-2 Collaboration
Laboratori Nazionali di Frascati dell'INFN, Via E. Fermi, 40, 00044 Frascati, Italy

Measurements of the muon magnetic anomaly performed at the Brookhaven Laboratory have reached a fractional accuracy of 0.54 10^{-6}. The final result differs from the Standard Model prediction by 3.2–3.6 standard deviations. Main uncertainty on the theoretical evaluations is due to hadronic loop contributions which, at low energy, are not calculable in perturbative QCD and are obtained from a dispersion integral over the measured hadronic cross section. The KLOE experiment at the DAΦNE ϕ-factory in Frascati was the first to exploit Initial State Radiation (ISR) processes for the precision measurement of the hadronic cross section below 1 GeV, that accounts for most (75%) of the hadronic contribution to the muon anomaly. In 2005 and 2008 KLOE published two measurements of the $e^+e^- \to \pi\pi\gamma$ cross section, with the ISR photon at small angle. An independent measurement with the photon emitted at large angle, to reach the dipion production threshold at s=0.1 GeV^2, was published in year 2011. Recently, a new analysis of KLOE data was performed, which directly derives the pion form factor from the bin–by–bin ratio of $e^+e^- \to \pi\pi\gamma$ to $e^+e^- \to \mu\mu\gamma$ cross sections. We discuss the final results of this analysis and present the comparison with our previous measurements. High-luminosity e^+e^- colliders at the GeV scale have been recognized to be an ideal environment to search for the U-boson in the Dark Force sector. We present the preliminary results of the U-boson search at KLOE using the $\mu\mu\gamma$ sample, from which an exclusion plot in the mass range from 600-1000 MeV is derived.

1 Introduction

The measurement of the muon magnetic anomaly, $a_\mu = (11\,659\,208.0 \pm 6.3) \times 10^{-10}$ [1], differs from Standard Model (SM) estimates by 3.2-3.6 standard deviations [2,3,4,5]. A recent evaluation [6] imposing model–dependent constraints on the pion form factor from other hadronic processes besides e^+e^- annihilation to $\pi\pi$ (annihilation to $\pi\gamma$, $\eta\gamma$, $\pi^+\pi^-\pi^0$, dipion spectrum from τ decays, meson radiative decays), finds an even larger discrepancy, between 4.7–4.9σ. The deviation could be a signal of New Physics as argued by many theoretical papers since 2001 [7,8]. New measurements of a_μ, aiming to a four-times-better precision, are expected at Fermilab [9] and J-PARC [10], for which it is important to confirm the evaluation of the hadronic corrections and possibly improve on their accuracy.

The main source of uncertainty for the SM calculation of a_μ is the leading hadronic vacuum polarization term [2,3], $\Delta^{\rm h,\,lo}a_\mu$. It is obtained from a dispersion integral [11,12] over the "bare" cross section $\sigma^0(e^+e^-\to \text{hadrons}(\gamma))$ that is derived from the physical cross section, inclusive of final state radiation, removing vacuum polarization (VP) effects and contributions due to additional photon emission in the initial state. The leading order hadronic contribution is $\sim$690 $\times$ 10^{-10} [2,3,4,5], to which the $e^+e^-\to\pi^+\pi^-(\gamma)$ process measured by KLOE is contributing about 75% of the value and 40% of the uncertainty.

2 Measurement of $\sigma(e^+e^- \to \pi^+\pi^-)$ at DAΦNE

We have published three measurements [13,14,15] of $\sigma(e^+e^-\to\pi^+\pi^-)$ for $0.1 < M^2_{\pi\pi} < 0.95\,\mathrm{GeV}^2$, with consistent results and a combined fractional uncertainty of about 1%.

The differential ISR cross section for the $e^+e^- \to \pi^+\pi^-\gamma$ final state is related to the dipion cross section $\sigma_{\pi\pi} \equiv \sigma(e^+e^- \to \pi^+\pi^-\gamma)$ [16]:

$$s\,\frac{\mathrm{d}\,\sigma(\pi^+\pi^-\gamma)}{\mathrm{d}\,s_\pi}\bigg|_{\mathrm{ISR}} = \sigma_{\pi\pi}(s_\pi)\;H(s_\pi, s), \tag{1}$$

where the radiator function H is computed from QED with complete NLO corrections[17,18,19,20,21].

Equation 1 is also valid for the di–muon final state with the same radiator function H. We can therefore determine $\sigma_{\pi\pi}$ from the ratio of the $\pi^+\pi^-\gamma$ and $\mu^+\mu^-\gamma$ differential cross sections:

$$\sigma^0(\pi^+\pi^-,\ s') = \frac{\mathrm{d}\sigma(\pi^+\pi^-\gamma,\ \mathrm{ISR})/\mathrm{d}s'}{\mathrm{d}\sigma(\mu^+\mu^-\gamma,\ \mathrm{ISR})/\mathrm{d}s'} \times \sigma^0(e^+e^- \to \mu^+\mu^-,\ s'). \tag{2}$$

Final state photon emission for both the $\pi^+\pi^-\gamma$ and $\mu^+\mu^-\gamma$ channels slightly modifies Eq. 2, and it has been considered in our analysis [22], where only events with photon emitted at small angle are used, as discussed in Refs. [14,15], a choice that results in a large enhancement of ISR with respect to FSR contribution.

The advantages of the ratio method are:

(i) the H function does not appear in Eq. 2. Therefore the measurement of $\sigma_{\pi\pi}$ is not affected by the related systematic uncertainty of 0.5% [17] ;

(ii) using the same data sample for the $\pi^+\pi^-\gamma$ and $\mu^+\mu^-\gamma$ events, there is no need for luminosity measurements;

(iii) vacuum polarization corrections and most other radiative corrections cancel in the ratio;

(iv) using the same fiducial volume, acceptance corrections to the $\pi^+\pi^-\gamma$ and $\mu^+\mu^-\gamma$ spectra almost cancel resulting in a small systematic uncertainty.

The pion form factor and $\Delta^{\pi\pi}a_\mu$ have been obtained using the $\pi\pi\gamma$ differential cross section of Ref. [14] and the $d\sigma_{\mu\mu\gamma}/ds_\mu$ measurement described in the following section.

3 The $\mu\mu\gamma$ Differential Cross Section

The analysis is based on an event selection that requires:

(i) reconstruction of at least two tracks of opposite sign, with origin at the interaction region (IP) and polar angle satisfying $50° < \theta < 130°$. The momenta satisfy $p_\perp > 160\,\mathrm{MeV}$ or $|p_z| > 90\,\mathrm{MeV}$, to ensure good reconstruction and efficiency;

(ii) polar angle $\theta_{\mu\mu}$ of the the dimuon system ($\mathbf{p}_{\mu\mu} = \mathbf{p}_+ + \mathbf{p}_-$) satisfying $|\cos\theta_{\mu\mu}| > \cos(15°)$;

(iii) computed mass for the two observed particles, as obtained from kinematical constraints assuming ISR $xx\gamma$ events, in the range $80 < m_x < 115\,\mathrm{MeV}$;

(iv) PID estimator, $L_\pm$, which uses time of flight information and energy deposit of each charged particle in the calorimeter, compatible with muon hypothesis at least for one track.

Residual $e^+e^-\gamma$, $\pi^+\pi^-\gamma$ and $\pi^+\pi^-\pi^0$ backgrounds are evaluated by fitting the observed m_x spectrum with a superposition of Monte Carlo simulation (MC) distributions describing signal and $\pi^+\pi^-\gamma$, $\pi^+\pi^-\pi^0$ backgrounds, and a distribution obtained from data for the $e^+e^-\gamma$ background. In the ρ mass region, the fractional $\pi^+\pi^-\gamma$ yield in the $\mu\mu\gamma$ acceptance region is about

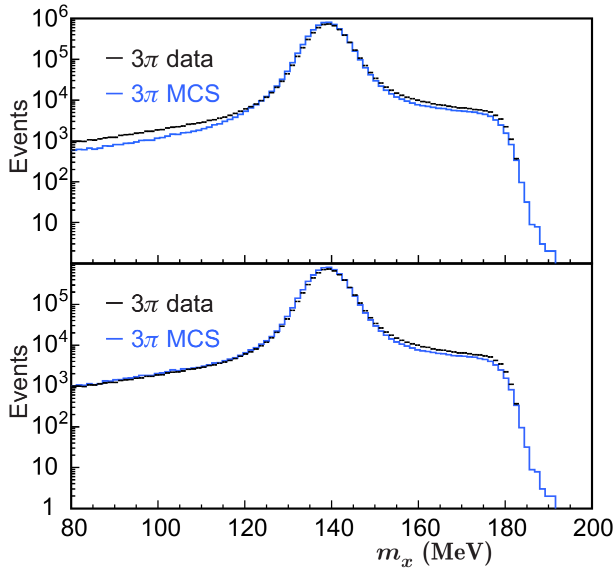

Figure 1: Data and MC m_x distributions for the $\pi^+\pi^-\pi^0$ control sample, before (upper) and after (lower) resolution correction, applied to improve the MC description of the low–energy m_x tail.

15% of the sample. To improve the MC description of the low–energy m_x tail of $\pi^+\pi^-\gamma$ events in the muon peak, we apply a data/MC resolution correction, function of s_μ. This correction is evaluated from a high–purity sample of $\phi \to \pi^+\pi^-\pi^0$ events, with the results shown in Fig. 1.

Contributions from $e^+e^- \to e^+e^-\mu^+\mu^-$ and $e^+e^- \to e^+e^-\pi^+\pi^-$ processes are evaluated using the `Nextcalibur` [23] and `Ekhara` [24] MC generators. After analysis cuts, the $e^+e^- \to e^+e^-\pi^+\pi^-$ process is found to be negligible, while the $e^+e^- \to e^+e^-\mu^+\mu^-$ background contribution is between 0.6% and 0.1%, in the low $M^2_{\mu\mu}$ region and is subtracted from the data spectrum. Systematic errors in the background subtraction include: (i) errors on the parameters from the fit procedure: these decrease monotonically from 0.7% to 0.1% with respect to s_μ; (ii) the uncertainty on the data/MC resolution corrections: about 1% in the ρ mass region, smaller at higher s_μ, negligible at lower s_μ values; (iii) the uncertainty on the $e^+e^- \to e^+e^-\mu^+\mu^-$ process: about 0.4% at low s_μ values, rapidly falling to 0.1% for $s_\mu > 0.5\,\mathrm{GeV}^2$. The correctness of the background estimate has been checked by two independent methods.

1) We perform a kinematic fit of the two track events assuming it is a $\mu\mu\gamma$ state. The χ^2 value obtained is used as discriminant variable, instead of m_x, in the fitting procedure described above;

2) we improve the π-μ separation by use of m_x, applying a quality cut on the helix fit for both tracks. This cut reduces the dipion background in the dimuon signal region by more than a factor of two.

The background fractions obtained for both cases are in good agreement with the standard procedure.

The differential $\mu^+\mu^-\gamma$ cross section is obtained from the observed event count N_{obs} and background estimate N_{bkg}, as

$$\frac{\mathrm{d}\,\sigma_{\mu\mu\gamma}}{\mathrm{d}\,s_\mu} = \frac{N_{\mathrm{obs}} - N_{\mathrm{bkg}}}{\Delta s_\mu}\,\frac{1}{\epsilon(s_\mu)\,\mathcal{L}} \tag{3}$$

where $\mathcal{L}$ is the integrated luminosity from Ref. [25] and $\epsilon(s_\mu)$ the selection efficiency. Figure 2, top, shows the measured $\mu^+\mu^-\gamma$ cross section compared with the QED calculations to NLO, using the MC code `Phokhara` [20]. Figure 2, bottom, shows the ratio between the two differential cross sections. The band indicates the systematic uncertainty, experimental and theoretical, of

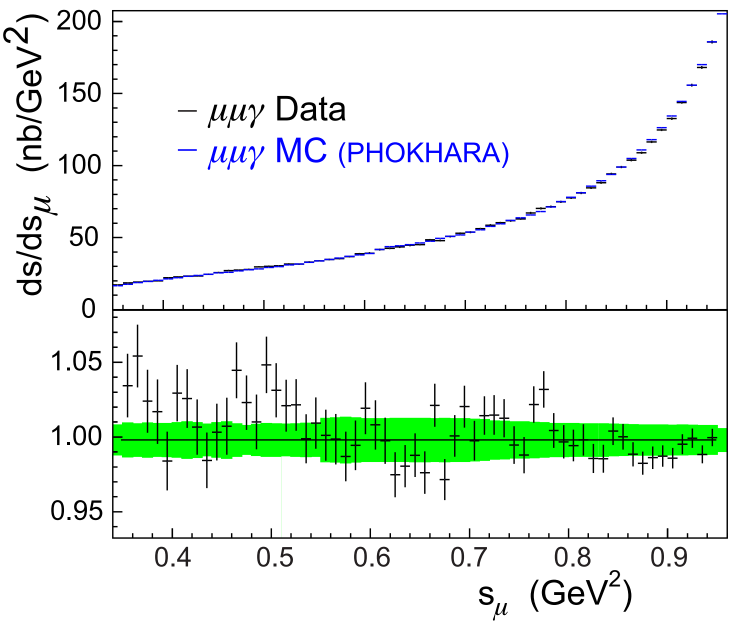

Figure 2: Top. Comparison of data and MC results for $\mathrm{d}\,\sigma_{\mu\mu\gamma}/\mathrm{d}\,s_\mu$. Bottom. Ratio of the two spectra. The band shows the systematic error.

Table 1: Comparison of the KLOE results on $\Delta^{\pi\pi}a_\mu$ in the interval $0.35 < M^2_{\pi\pi} < 0.85\,\mathrm{GeV}^2$ common to all of the independent measurements.

Analysis	$\Delta^{\pi\pi}a_\mu \cdot 10^{10}$ $[0.35 < M^2_{\pi\pi} < 0.95\,\mathrm{GeV}^2]$
$\pi\pi\gamma$ to $\mu\mu\gamma$ ratio	$377.4 \pm 1.1_{\mathrm{stat}} \pm 2.7_{\mathrm{sys+th}}$
$\sigma(\pi\pi\gamma)$ (abs.); small–angle γ	$379.6 \pm 0.4_{\mathrm{stat}} \pm 3.3_{\mathrm{sys+th}}$
$\sigma(\pi\pi\gamma)$ (abs.); large–angle γ	$376.6 \pm 0.9_{\mathrm{stat}} \pm 3.3_{\mathrm{sys+th}}$

the measured cross section. The average ratio, using only statistical errors, is 0.9981 ± 0.0015, showing a good agreement within the quoted systematic uncertainty.

4 The Hadronic Vacuum Contribution to a_μ

From the bin–by–bin ratio between our published [14] $\pi^+\pi^-\gamma$, and the $\mu^+\mu^-\gamma$ differential cross sections described above, we obtain the bare cross section $\sigma^0_{\pi\pi(\gamma)}$ (inclusive of FSR, with VP effects removed) which is used in the dispersion integral for computing $\Delta^{\pi\pi}a_\mu$. Figure 3 shows the $\pi^+\pi^-\gamma$ and $\mu^+\mu^-\gamma$ event spectra after background subtraction and data/MC corrections (top) and the bare cross section $\sigma^0_{\pi\pi(\gamma)}$ (bottom). Systematic uncertainties on $\sigma^0_{\pi\pi(\gamma)}$ are smaller than the individual uncertainty on $\pi\pi\gamma$ and $\mu\mu\gamma$ due to correlation between the two measurements [22].

The dispersion integral for $\Delta^{\pi\pi}a_\mu$ is computed as the sum of the values for $\sigma^0_{\pi\pi(\gamma)}$ times the kernel $K(s)$, times $\Delta s = 0.01\,\mathrm{GeV}^2$:

$$\Delta^{\pi\pi}a_\mu = \frac{1}{4\pi^3}\int_{s_{min}}^{s_{max}} \mathrm{d}\,s\,\sigma^0_{\pi\pi(\gamma)}(s)\,K(s)\ , \tag{4}$$

where the kernel is given in in Ref. [12].

Eq. 4 gives $\Delta^{\pi\pi}a_\mu = (385.1 \pm 1.1_{\mathrm{stat}} \pm 2.6_{\mathrm{exp}} \pm 0.8_{\mathrm{th}}) \times 10^{-10}$ in the interval $0.35 < M^2_{\pi\pi} < 0.95\,\mathrm{GeV}^2$, that is consistent with our previous measurements as shown in Tab. 1.

This result, with comparable total experimental uncertainty and a theoretical error reduced by about 70% with respect to our previous measurements [14], confirms the current discrepancy between the SM prediction and the experimental value of a_μ.

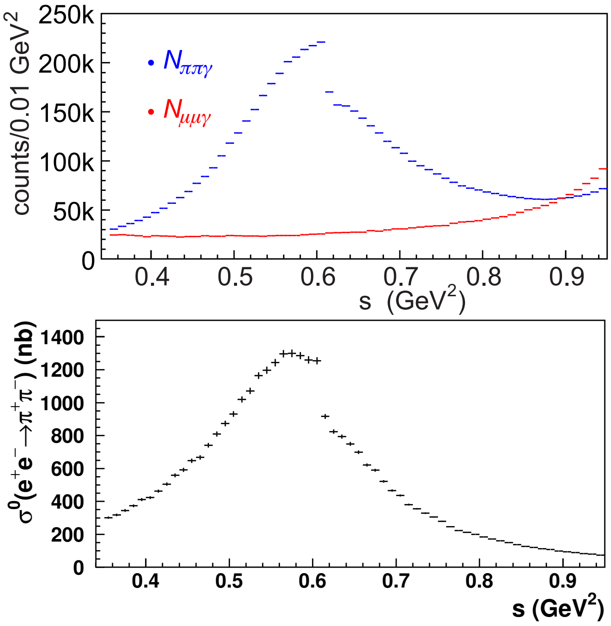

Figure 3: Square–invariant–mass distributions of $\pi^+\pi^-\gamma$ (higher counts from 0–0.9 GeV^2) and $\mu^+\mu^-\gamma$ (lower counts from 0–0.9 GeV^2) events after background subtraction and data/MC corrections (top); the bare cross section from the $\pi^+\pi^-\gamma/\mu^+\mu^-\gamma$ ratio (bottom).

5 Searches for the U–boson

Some models of physics beyond the SM predict the existence of light neutral vector particles (called U–bosons) mediator of new gauge interactions under which ordinary matter is uncharged [26,27]. Motivated by astrophysical arguments, their mass, M_U, is expected to be of order 1 GeV or lighter [28,29]. Coupling of SM particles with the U is possible via kinetic mixing between the U and the ordinary photon [30], regulated by a dimensionless parameter ϵ, expected to be of order $\epsilon \sim 10^{-3}$ or lower.

These new particles can be observed as sharp resonances at M_U in the invariant mass distribution of charged lepton or pion pairs in reactions of the type $e^+e^- \to l^+l^-\gamma$ or $V \to Pl^+l^-$, where V (P) stands for any vector (pseudoscalar) meson, and $l^\pm$ can be muons, electrons or charged pions.

KLOE has searched for U boson production in both modes, using $\phi \to \eta e^+e^-$ events (a), and $e^+e^- \to \mu^+\mu^-\gamma$ events (b).

As for reactions (a), a first paper has been published [31] in which the presence of the η meson was tagged using its $\pi^+\pi^-\pi^0$ decays; a second paper has been subsequently issued [32] in which also the $3\pi^0$ decay channel of the η was used. In both cases a sample corresponding to 1.7 fb^{-1} of data at the ϕ peak was used; no evidence of the U boson is found, and the exclusion plot, in the interval $30 < M_U < 400$ MeV, has been obtained (Fig. 4).

Reaction (b) was studied on the sample used for the measurement of the ratio, $R = \sigma(e^+e^- \to \pi^+\pi^-)/\sigma(e^+e^- \to \mu^+\mu^-)$, presented in the previous section, exploiting the precision MC simulation of the QED process $e^+e^- \to \mu\mu\gamma$ reported in Fig. 2. The exclusion plot is obtained using the CL$_S$ technique. The preliminary result shown in Fig. 4 covers the mass region $600 < M_U < 1000$ MeV and is currently being extended to 500 MeV.

References

1. G. W. Bennett et al. *Phys. Rev.*, D73:072003, 2006.
2. J. P. Miller, E. De Rafael, and B. Lee Roberts. *Rept. Prog. Phys.*, 70:795, 2007.
3. F. Jegerlehner and A. Nyffeler. *Phys. Rept.*, 477:1–110, 2009.

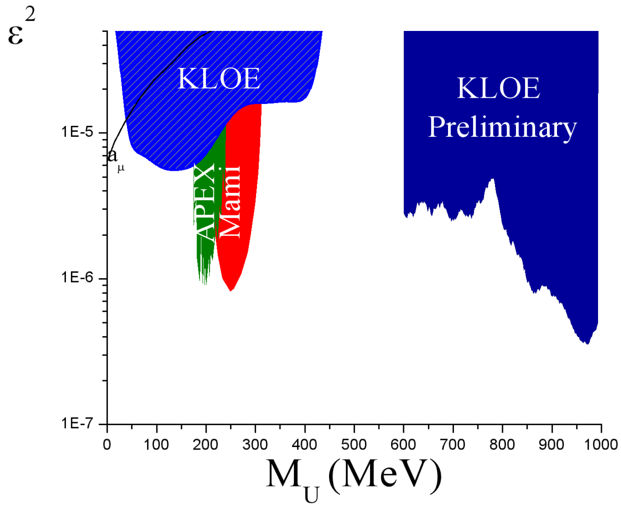

Figure 4: KLOE-2 limit in the plane M_U–ϵ^2. Results are shown for the $\phi \to \eta e^+ e^-$ analysis and for the $e^+e^- \to \mu^+\mu^-\gamma$ one. The results from the APEX and MAMI-A1 experiments are also shown

4. M. Davier, A. Hoecker, B. Malaescu, and Z. Zhang. *Eur. Phys. J.*, C71:1515, 2011.
5. K. Hagiwara et al. *J. Phys.*, G38:085003, 2011.
6. M. Benayoun et al. $arXiv$:1210.7184[$hep-ph$]. 2012.
7. A. Czarnecki and W. J. Marciano. *Phys. Rev.*, D64:013014, 2001.
8. J. P. Miller et al. *Annual Rev. of Nucl. and Part. Sc.*, 62(1):237–264, 2012.
9. R. M. Carey. *AIP Conf.Proc.*, 1182:678–681, 2009.
10. J. Imazato. *Nucl. Phys. Proc. Suppl.*, 129:81–87, 2004.
11. C. Bouchiat and L. Michel. *J. Phys. Radium*, 22:121, 1961.
12. B.E. Lautrup, A. Peterman, and E. De Rafael. *Nuovo Cim.*, A1:238–242, 1971.
13. F. Ambrosino et al. *Phys. Lett.*, B700:102–110, 2011.
14. F. Ambrosino et al. *Phys. Lett.*, B670:285–291, 2009.
15. A. Aloisio et al. *Phys. Lett.*, B606:12–24, 2005.
16. S. Binner, Johann H. Kuhn, and K. Melnikov. *Phys. Lett.*, B459:279–287, 1999.
17. G. Rodrigo, H. Czyz, J. H. Kuhn, and M. Szopa. *Eur. Phys. J.*, C24:71–82, 2002.
18. H. Czyz, A. Grzelinska, J. H. Kuhn, and G. Rodrigo. *Eur. Phys. J.*, C27:563–575, 2003.
19. H. Czyz, A. Grzelinska, J. H. Kuhn, and G. Rodrigo. *Eur. Phys. J.*, C33:333–347, 2004.
20. H. Czyz, A. Grzelinska, J. H. Kuhn, and G. Rodrigo. *Eur. Phys. J.*, C39:411–420, 2005.
21. S. Actis et al. *Eur. Phys. J.*, C66:585–686, 2010.
22. P. Lukin et al. http://www.lnf.infn.it/kloe2/tools/getfile.php?doc_fname=K2PD-6.pdf&doc_ftype=docs.
23. F. A. Berends et al. *Comput. Phys. Commun.*, 136:148–172, 2001.
24. H. Czyz and E. Nowak-Kubat. *Phys. Lett.*, B634:493–497, 2006.
25. F. Ambrosino et al. *Eur. Phys. J.*, C47:589–596, 2006.
26. P. Fayet. *Phys. Lett.*, B95:285, 1980.
27. B. Batell, M. Pospelov, and A. Ritz. *Phys. Rev.*, D80:095024, 2009.
28. N. Arkani-Hamed and N. Weiner. *JHEP*, 12:104, 2008.
29. M. Pospelov, A. Ritz, and M. B. Voloshin. *Phys. Lett.*, B662:53–61, 2008.
30. B. Holdom. *Phys. Lett.*, B166:196, 1986.
31. F. Archilli et al. *Phys. Lett.*, B706:251–255, 2012.
32. D. Babusci et al. *Phys. Lett.*, B720:111, 2013.